Novel Sensing Methodology for Initial Alignment Using MmWave Phased Arrays

Rohan R. Pote
ECE Department, UC San Diego

Bhaskar D. Rao
ECE Department, UC San Diego

2023 57th Asilomar Conference on Signals, Systems, and Computers | 979-8-3503-2574-4/23/$31.00 ©2023 IEEE | DOI: 10.1109/IEEECONF59524.2023.10476851

***Abstract*—A novel sensing approach for the single radio frequency (RF) chain millimeter wave systems is proposed. The sensing strategy is inspired from synthetic aperture radar systems, and synthesizes a *virtual array manifold* vector using a single phased array over temporal measurements. The geometry of the virtual array can be controlled enabling synthesis of both a virtual uniform linear array (ULA) and a virtual sparse linear array starting from a large physical array. Moreover, the proposed sensing can be realized using conventional phased array/analog combiner. Several design parameters of the sensing scheme provide flexibility and are discussed including their impact on initial alignment. The proposed sensing approach allows for a rich set of options for inference. Candidate detection and estimation algorithms are presented and their performance is evaluated.**

I. Introduction

An ever-increasing number of user devices are getting connected to cellular networks with the demand for data per device rising rapidly. Millimeter wave (mmWave) spectrum allocation is envisioned to support this demand and enable many new use cases such as industrial-IoT, virtual and augmented reality, biomedical applications, and non-terrestrial networks in the beyond 5G (B5G) and 6G cellular networks [1]. The challenges to successfully establish mmWave communication link include large propagation losses and sparse multipath environment. Owing to the large propagation losses in mmWave channel, massive MIMO technology and beamforming gain become crucial to achieve reliable and low latency communication. On the other hand, the specular nature of the mmWave channel renders it to be sparse and requires accurate Beam Alignment (BA). This challenge is only further exacerbated by the narrow beamwidths and consequent large codebook size due to the large antenna array dimensions.

Reducing the BA duration is a critical and an active area of research. Hardware cost also impacts the ability of the transceivers to sense the mmWave channel. The large number of antenna elements are typically supported by only a few Radio Frequency (RF) chains [2], and thus necessitates for a low-dimensional projection of the received signal at the antennas. Beam alignment using such a low-dimensional signal is a challenging problem. There is a need to build a better sensing approach to achieve significant reduction in BA duration that can exploit the array geometry and channel characteristics under the hardware constraints. The need is accurately captured with the recent surge in research related to Integrated Sensing and Communication (ISAC) wherein sensing and communication services co-exist to reduce power consumption, improve spectral efficiency and allow for hardware-reuse [3].

In this work we address the BA problem when only a single RF chain is available. A novel sensing approach is proposed that allows to beamform in a Region of Interest (RoI) while simultaneously capturing *rich* information about the sparse mmWave channel. The contributions of this work are as follows:

- A novel sensing methodology, inspired from Synthetic Aperture Radar (SAR), is proposed for the single RF chain mmWave systems. Under the proposed sensing approach, a virtual Uniform Linear Array (ULA) manifold is synthesized over temporal measurements. Extension to construct a virtual arbitrary array geometry such as Sparse Linear Array (SLA) is also discussed.
- We provide candidate estimation and detection algorithms that infer the dominant beam Direction-of-Arrival (DoA) based on measurements using proposed sensing. The presented algorithms demonstrate the many options for inference enabled by the proposed sensing scheme. It is also highlighted how proposed sensing can be incorporated within other BA algorithms with the help of hierarchical Posterior Matching (hiePM) technique proposed in [4].

Numerical results are provided that highlight the benefit from using proposed sensing over conventional schemes in literature. *Notations*: $(.)^c$ denotes complex conjugate operation, and $[M] = \{0, 1, \ldots, M-1\}, M \in \mathbb{Z}^+$.

II. Problem Statement and Proposed Sensing

We consider a receiver (base station or user equipment) equipped with a ULA of size N and a single RF chain. We assume a flat fading channel, with a single dominant path between the transmitter and receiver. We further assume that the channel remains coherent within the training duration due to low receiver mobility.

A. Problem Statement

The received signal at the antennas at instant l, $\mathbf{x}_l \in \mathbb{C}^N$, is given by

$$\mathbf{x}_l = \sqrt{P_s}\alpha\boldsymbol{\phi}_N(u) + \bar{\mathbf{n}}_l, \quad 0 \le l < L, \tag{1}$$

where L denotes the total training duration. $P_s\ (>0)$ denotes the combined contribution of transmitted power and the large-scale fading (path loss and shadowing), $\alpha \in \mathbb{C}$ is the *unknown* small-scale fading coefficient. Since the transmitted symbol is

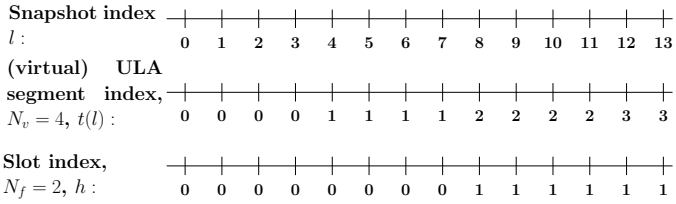

Fig. 1. A (virtual) ULA segment of aperture size $N_v = 4$ is created using 4 snapshots. The beamformer is adapted once every slot to improve signal-to-noise ratio (SNR), here slot size is $N_f = 2$.

known, it can be easily absorbed within the signal term of $\mathbf{x}_l$ in (1). Thus, we assume the transmitted symbol value to be 1 without loss of generality. $\boldsymbol{\phi}_N(u)$ is the array manifold or response vector for an incoming narrowband signal along the angle u; $u = \sin\theta, u \in [-1, 1)$, where $\theta \in [-\frac{\pi}{2}, \frac{\pi}{2})$ denotes physical DoA. Noise $\bar{\mathbf{n}}_l \in \mathbb{C}^N$ is distributed as $\mathcal{CN}(\mathbf{0}, \sigma_n^2\mathbf{I})$ and i.i.d. over time. Since there is a single RF chain, the received signal is processed using an analog combiner, $\mathbf{w}_l \in \mathbb{C}^N$. The output, $y_l \in \mathbb{C}$, available for inference is given by

$$\begin{aligned} y_l = \mathbf{w}_l^H \mathbf{x}_l &= \sqrt{P_s}\alpha \mathbf{w}_l^H \boldsymbol{\phi}_N(u) + \mathbf{w}_l^H \bar{\mathbf{n}}_l \\ &= \sqrt{P_s}\alpha \mathbf{w}_l^H \boldsymbol{\phi}_N(u) + n_l. \end{aligned} \tag{2}$$

The goal is to design $\mathbf{w}_l$ and infer u; $\mathbf{w}_l$ can be adapted over time to improve the inference. For a ULA with $\lambda/2$ inter-element spacing[1], where λ denotes the wavelength of the received signal, we have

$$\boldsymbol{\phi}_N(u) = [1 \ \exp(j\pi u) \ \cdots \ \exp(j\pi(N-1)u)]^T. \tag{3}$$

In this paper, we consider the ULA geometry for easier exposition of ideas. However, these ideas can be extended to planar geometries as well, such as uniform rectangular arrays [5]. Next, we describe the proposed sensing scheme which provides a high-level structure to the beamformer, $\mathbf{w}_l$. We refer to this sensing methodology as Synthesis of Virtual Array Manifold (SVAM).

B. Synthesis of Virtual Array Manifold (SVAM) Sensing

We propose a novel sensing approach inspired by synthetic aperture radar used in remote sensing and automotive radar [6]. In typical SAR systems, the sensor motion allows synthesis of larger aperture than physical antenna, which helps to improve resolution. In this work, we mimic the sensor motion by designing $\mathbf{w}_l$ accordingly. We exploit the coherence interval to synthesize virtual apertures *over time*. An important consequence is that, such measurements preserve phase information from the physical antenna, which captures rich information about the DoA of the incoming signal. The proposed sensing can be applied more broadly to multi-path angles. Moreover, leveraging the complex exponential structure present at the combiner output $y_l, l \in [L]$, it is possible to apply an *unlimited* number of digital filters on these measurements.

1) Constructing a Virtual ULA with $\lambda/2$ Inter-element Spacing: Let N_v ($\leq N$) denote the aperture size of the *virtual* ULA we wish to create. We assume that the total training duration, L, is divisible by N_v for simplicity. Let $t(l) = \text{floor}(l/N_v)$ denote[2] the virtual ULA segment index (see Fig. 1). We design a beamformer of size $M = N - N_v + 1$ denoted by $\mathbf{f}_{t(l)} \in \mathbb{C}^M$, such that $\|\mathbf{f}_{t(l)}\|_2 = 1$. Initially the beamformer is designed to span a Region of Interest (RoI) and may be adapted over time. Such RoI can be used to incorporate any prior information available about the DoA. The analog combiner at instant l is given by

$$\mathbf{w}_l = \begin{bmatrix} \mathbf{0}^T_{\text{mod}(l,N_v)} & \mathbf{f}^T_{t(l)} & \mathbf{0}^T_{N_v - \text{mod}(l,N_v)-1} \end{bmatrix}^T. \tag{4}$$

Thus, within a segment duration, the beamformer slides along the antenna aperture and performs convolution in space. In contrast to the work in [7], here only a single RF chain is available and thus a virtual ULA segment is synthesized over time. Let

$$\beta_{t(l)}(u) = \mathbf{f}^H_{t(l)} \boldsymbol{\phi}_M(u), \tag{5}$$

denote the complex gain of the beamformer along the angle u. The signal y_l post-combining can be expressed as

$$y_l = \mathbf{w}_l^H \mathbf{x}_l = \sqrt{P_s}\alpha\beta_{t(l)}(u) \cdot \exp\{j\pi u \text{mod}(l, N_v)\} + n_l. \tag{6}$$

Note that, the complex gain $\beta_{t(l)}(u)$ does not change within a segment, but '$\exp\{j\pi u \text{mod}(l, N_v)\}$' varies within the segment.

Remark 1. The beamforming gain, measured in terms of $|\beta_{t(l)}(u)|^2$, in the passband depends primarily on the beamwidth of the beamformer, $\mathbf{f}_{t(l)}$. For an ideal beamformer design, the gain in the beamformer passband corresponding to a beamwidth of $\frac{2}{R}, R \geq 1$, in u-space is given by $|\beta_{t(l)}(u)|^2 = R$. As the beamformer size, M, increases the beamformer response approaches the ideal response.

We drop the notation of dependence of t on l for simplicity. We stack the measurements within a segment to form $\mathbf{y}_t = \begin{bmatrix} y_{tN_v} & y_{tN_v+1} & \cdots & y_{(t+1)N_v-1} \end{bmatrix}^T, t \in [L/N_v]$ (see Fig. 1) as

$$\begin{aligned} \mathbf{y}_t &= \sqrt{P_s}\alpha\beta_t(u) [1 \ \exp j\pi u \ \cdots \ \exp j(N_v - 1)\pi u]^T + \mathbf{n}_t \\ &= \sqrt{P_s}\alpha\beta_t(u)\boldsymbol{\phi}_{N_v}(u) + \mathbf{n}_t. \end{aligned} \tag{7}$$

We identify the following design parameters: a) $N_v \in \{1, 2, \ldots, N\}$, the virtual ULA size, and b) beamformer, $\mathbf{f}_t$ design, which includes the beam direction and beam width. $N_v = 1$ reduces to the conventional beam design. Thus, the proposed sensing strategy includes the methodology adopted for sensing in [4], [8] as a special case. The hierarchical codebook in [8] designed using a least squared error criterion imposes a constant amplitude and phase in the passband. The inference is improved by relaxing the constant phase requirement in the passband. Thus, in this work we design the beamformers, $\mathbf{f}_t$, as *linear*-phase Finite Impulse Response (FIR) filter using the Parks-McClellan algorithm [9].

[1] $\lambda/2$ inter-element spacing prevents ambiguity in angular estimation.

[2] $\text{floor}(\cdot)$ denotes the floor function.

Remark 2. It is important to highlight the significance of the proposed sensing methodology. Given just two measurements, it is possible to construct a virtual ULA under the proposed sensing with $N_v = 2$. This is equivalent to a *single* snapshot measurement from a physical array of size 2. Owing to the rich (array) geometrical information preserved in the measurements, it is thus possible to *estimate* the dominant path DoA in a *gridless* manner using existing techniques [10]–[12]. In contrast, the beam scan operation using $N_v = 1$ requires as many measurements as the codebook size to *detect* the DoA.

2) Constructing a Virtual Sparse Linear Array: The construction presented in the previous subsection can be extended to form virtual ULAs with more than $\lambda/2$ spacing[3]. More generally, a Sparse Linear Array (SLA) can also be realized as the virtual array geometry, for example, minimum redundancy arrays [13] or nested arrays [14]. These can help to increase the virtual aperture and improve resolution for the same segment duration. Let N_v denote the number of antenna elements in the virtual SLA we wish to construct over time. Let $\mathbb{P} = \{P_i : 0 \leq P_i < N, P_i \in \mathbb{Z}, i \in [N_v]\}$ denote the set of sensor positions in the SLA ordered in an increasing manner; $P_0 = 0$, without loss of generality. We design a beamformer, $\mathbf{f}_t$, of length $M = N - P_{N_v-1}$. The analog combiner at time l, in the case of SLA, is given by

$$\mathbf{w}_l = \begin{bmatrix} \mathbf{0}^T_{P_{\mathrm{mod}(l,N_v)}} & \mathbf{f}_t^T & \mathbf{0}^T_{N-M-P_{\mathrm{mod}(l,N_v)}} \end{bmatrix}^T. \quad (8)$$

Using identical notation to describe the complex gain, $\beta_t(u)$, as in (5), the signal y_l post-combining can be expressed as

$$y_l = \mathbf{w}_l^H \mathbf{x}_l = \sqrt{P_s}\alpha\beta_t(u) \cdot \exp\left(j\pi u P_{\mathrm{mod}(l,N_v)}\right) + n_l. \quad (9)$$

Note that (9) generalizes (6) for the SLA case. Finally, the measurements within the t-th SLA segment can be stacked as

$$\begin{aligned}\mathbf{y}_t &= \sqrt{P_s}\alpha\beta_t(u)[1 \ \exp(j\pi P_1 u) \cdots \exp(j\pi P_{N_v-1} u)]^T + \mathbf{n}_t \\ &= \sqrt{P_s}\alpha\beta_t(u)\mathbf{S}_{\mathbb{P}}\boldsymbol{\phi}_N(u) + \mathbf{n}_t, \end{aligned} \quad (10)$$

where $\mathbf{S}_{\mathbb{P}} \in \mathbb{R}^{N_v \times N}$ is a binary sampling matrix given by

$$[\mathbf{S}_{\mathbb{P}}]_{m,n} = \begin{cases} 1 & \text{if } n = P_m \\ 0 & \text{otherwise} \end{cases}, m \in [N_v], n \in [N]. \quad (11)$$

In the remainder of the work, we focus on the virtual ULA with $\lambda/2$ spacing-based sensing for ease of exposition, but the ideas presented can be easily extended to the virtual SLA case. The proposed design for $\mathbf{w}_l$ in (6) and (9) may be realized using a pair of phase shifters to form arbitrary modulus for the beamformer coefficients (see Theorem 1 in [15]).

III. Various Inference Procedures Enabled by the Novel SVAM Sensing

We begin by first noting that in the absence of prior on both α and u we need at least two snapshots to make meaningful inference on (α, u), even if the SNR is infinite. Moreover, if N_v is set to one, then the filter design over the two snapshots must have different magnitude or phase response (see Chapter 1, Section 4.1 in [16]). We select $N_v \geq 2$ in this work. We highlight that both the synthetic aperture size and virtual array geometry can be adapted over time, although we do not explore this further in this work. In this section, we present three different options for inferring u using SVAM measurements as described in the previous section.

A. Fixed Interval Beam Adaptation

In order to combat noise we can construct multiple virtual ULA segments keeping the beamfomer design $\mathbf{f}_t$ fixed. We refer to this duration as a *slot* (see Fig. 1). In other words, $\mathbf{f}_t$ is adapted once after each slot. Let N_f denote the slot size, indicating the number of virtual ULA segments contained in one slot. We infer u based on the following average statistic $(h \in [L/(N_v N_f)])$

$$\tilde{\mathbf{y}}_h = \frac{1}{N_f} \sum_{t=hN_f}^{(h+1)N_f-1} \mathbf{y}_t. \quad (12)$$

The slot duration may be adapted over time depending on SNR. Such an adaptive strategy is explored in [16]. The modified hiePM algorithm discussed in the next subsection is another example wherein the slot duration is adapted dynamically, although hiePM [4] assumes that α is known.

1) Detection Strategy: Owing to the complex exponential signal component in (7), it is possible to apply much less restrictive *digital* filter to infer u. We use this feature explicitly within the detection strategy. By framing a detection question, we hope to enable the overall framework to operate in low SNR regime. We divide the RoI into P partitions and design P beamformers $\mathbf{f}_{h,p}^{\mathrm{det}} \in \mathbb{C}^{N_v}, p = \{1, \ldots, P\}$; each beam focuses in one such partition. The algorithm then compares power in the P narrow partitions within the RoI

$$p_h^{\mathrm{DET}} = \arg\max_p \left| \left(\mathbf{f}_{h,p}^{\mathrm{det}}\right)^H \tilde{\mathbf{y}}_h \right|^2. \quad (13)$$

The P partitions may be steered to identify more meaningful partitions. This is implemented in Section IV. Although a large P allows to design narrow beamwidths with higher beamforming gain, it may also increase the misdetection probability.

2) Estimation Strategy: We model the unknowns (α,u) as deterministic variables. Note that both can be modeled as stochastic variables, especially if additional prior is available. Such a stochastic modeling for estimation is considered in [16]. For a fixed u', the maximum likelihood estimation (MLE) of α gives

$$\alpha_h^{\mathrm{MLE}}(u') = \frac{1}{\sqrt{P_s}} \frac{\boldsymbol{\phi}_{N_v}(u')^H \left(\sum_{h'=0}^{h} \beta^c_{h'N_f}(u')\tilde{\mathbf{y}}_{h'}\right)}{\|\boldsymbol{\phi}_{N_v}(u')\|^2 \sum_{h'=0}^{h} |\beta_{h'N_f}(u')|^2}. \quad (14)$$

Let $g_h(u') = \sum_{h'=0}^{h} |\beta_{h'N_f}(u')|^2$ denote the cumulative beamforming gain upto slot h. The MLE optimization problem reduces to

$$u_h^{\mathrm{MLE}} = \arg\max_{u'} \left| \frac{\boldsymbol{\phi}_{N_v}(u')^H}{\|\boldsymbol{\phi}_{N_v}(u')\|} \left(\sum_{h'=0}^{h} \frac{\beta^c_{h'N_f}(u')}{\sqrt{g_h(u')}} \tilde{\mathbf{y}}_{h'} \right) \right|^2. \quad (15)$$

[3]Any ambiguity in angular estimation can be resolved if the RoI is an appropriate fraction of the spatial region.

The above optimization uses the well-known *matching* objective. The presence of the manifold vector $\boldsymbol{\phi}_{N_v}(u')$ highlights the importance of the virtual geometry we synthesize; it decides the resolution. Sparse geometries such as nested arrays [14] can help to synthesize large apertures in *fewer snapshots*[4].

Algorithm 1: Beam Alignment Using SVAM Sensing

Result: $u_{\text{final}} = u^*_{L/(N_v N_f)-1}$
Input: $L, N_v, N_f, (P$ for detection, G for estim.$)$
Initialize: $\mathbf{f}_0$ spans RoI
for $l := 0$ to $\mathrm{L}-1$ **do**
  $y_l = \mathbf{w}_l^H \mathbf{x}_l$ *(New measurement, $\mathbf{w}_l$ as in (4))*
  if $\mathrm{mod}(l+1, N_v) = 0$ **then**
    $t := (l+1)/N_v - 1$ *(ULA segment index)*
    Vectorize measurements to form $\mathbf{y}_t$ as in (7)
    if $\mathrm{mod}(l+1, N_v N_f) = 0$ *(New slot)* **then**
      $h := (l+1)/(N_v N_f) - 1$ *(slot index)*
      Compute $\tilde{\mathbf{y}}_h$ as in (12)
      $u_h^* :=$ (outcome of detection (III-A1) OR estimation (III-A2))
      $u^{\mathrm{BW}} := u^{\mathrm{BW}}/2$
      $\mathbf{f}_{(h+1)N_f}$: Parks-McClellan Filter Design $\left(u_h^*, u^{\mathrm{BW}}\right)$
    else
      $\mathbf{f}_{t+1} = \mathbf{f}_t$
    end
  end
end

The beam direction is adapted based on the inference in the previous slot. The beamwidth is reduced by a deterministic amount (e.g., $0.5\times$previous beamwidth in Section IV). The suggested BA procedure is summarized in Alg. 1. A more principled approach may be to guide the beamwidth using bounds on variance of estimation.

B. HiePM-based Dynamic Beam Adaptation: A Plug-and-Play SVAM Sensing Approach

The hiePM algorithm [4] processes each new snapshot and updates the beamformer based on the current estimate of the posterior density on the unknown DoA. Note that it assumes that α is known. To incorporate the proposed sensing, one approach is to update the beamformer after every N_v snapshots, where N_v denotes the size of the virtual ULA. Within each N_v interval, a SVAM beamformer, $\mathbf{f}_t$, is designed; $\mathbf{f}_t$ is simply a codeword from the hierarchical codebook that satisfies the selection criteria within hiePM framework. The beamfomer (of physical antenna aperture size, N) for N_v snapshots within this interval is constructed as in (4). The remainder steps in Algorithm 1 in [4] are compatible with the proposed sensing.

The impact of the modification can be understood in the following manner. The hiePM strategy in [4] may repeat the same beamformer multiple times until the posterior condition triggers a new beamformer. While it repeats the beamformer, it gains only in terms of SNR. In the proposed sensing, the shifted spatial combining mimics a convolution operation and aims to achieve both, a SNR boost and additional angular information in the phase.

[4]The beamformer, $\mathbf{f}_t$, length reduces with aperture length, and thus there exists a tradeoff between virtual aperture size and beamformer design quality.

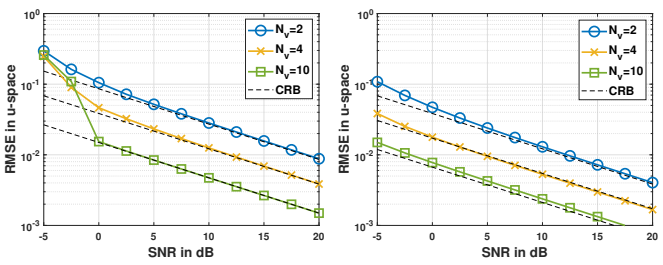

(a) Total snapshots, $L = 20$ (b) Total snapshots, $L = 100$

Fig. 2. (a) and (b) plot RMSE as a function of snapshots using non-adaptive beamformer and root-MUSIC, when source lies in $(-0.6, 0.6)$ in u-space.

IV. Numerical Results

We numerically analyze the benefit of proposed SVAM sensing over conventional beamforming when multiple snapshots are taken. We evaluate the performance under two scenarios namely, i. non-adaptive beamformer ii. adaptive beamformer. In the former scenario, the proposed SVAM sensing allows using classical array processing algorithms such as MUSIC and ESPRIT, as it constructs a virtual array manifold from a single phased array measurements. For the latter scenario, we explore both low snapshot and low SNR regimes as the beamformer is allowed to adapt over time. Here, we evaluate the performance of proposed sensing under different assumptions on knowledge of α. We implement different inference and beam alignment procedures that utilize the measurements under SVAM sensing. These procedures include the schemes discussed in Section III. We also benchmark the performance with the hiePM algorithm in [4]. The physical antenna size considered in this section is $N = 64$. The main metric employed for comparison is the root mean squared error (RMSE) computed in u-space as $\text{RMSE} = \sqrt{\frac{1}{Q}\sum_{q=1}^{Q}(\hat{u}_q - u_q)^2}$; Q denotes the total number of random trials.

A. SVAM study with Non-Adaptive Beamformer

1) RMSE as a function of SNR using root-MUSIC: The path angle lies in the range $(-0.6, 0.6)$ in u-space. The beamformer $\mathbf{f}_t$ is designed to span this RoI. Fig. (2) (a) plots the RMSE as a function of SNR when $L = 20$ total snapshots are available. Since the beamformer is not adapted, clearly constructing a larger virtual ULA performs better as SNR increases. This is expected as larger virtual apertures can help to carry more information about the unknown path angle. Fig. (2) (b) plots a similar curve when the total number of snapshots is $L = 100$. The results are averaged over $Q = 200$ random trials for both the plots. The plots clearly highlight the significance of SVAM sensing. With $N_v = 1$ and without the knowledge

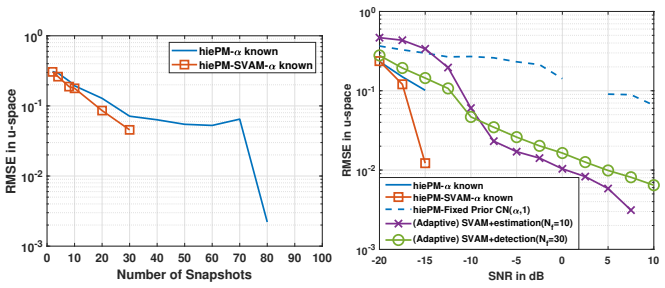

(a) SNR=-10 dB (b) Total snapshots, $L = 120$

Fig. 3. (a) RMSE as a function of snapshots using two variants of hiePM algorithm. (b) RMSE over SNR in dB using different adaptive algorithms.

of α, the measurements are uninformative of path angle and α simultaneously. With $N_v > 1$, we can see both improved estimation performance and improved lower bound on its variance, clearly indicating the benefit from constructing larger virtual apertures. However, note that when beamformer, $\mathbf{f}_t$, is allowed to adapt, higher virtual array size may not necessarily result in better performance. This is explored in [16].

B. SVAM study with Adaptive Beamformers

We assume that the DoA, u, lies in between $[0, 1)$ i.e., RoI is $\frac{1}{2}$ of the entire space. The path angle lies on a uniform angular grid of size $G = 64$ in RoI. The different algorithms locate the path angle on the same grid as the true path angle.

1) RMSE as a function of number of snapshots: Fig. 3 (a) plots the RMSE (over $Q = 200$ realizations) as a function of number of snapshots. The SNR is set to -10 dB. Both the curves assume α is known. The red curve uses the proposed SVAM sensing with $N_v = 4$ (as described in Section III-B) as opposed to the sensing methodology in hiePM [4]. The posterior computations and the beamformer design are similar to hiePM. As observed in the plot, using the proposed SVAM sensing, the algorithm requires fewer snapshots for the posterior mode to align with the ground truth angle. In this experiment, 40 snapshots are sufficient for the proposed SVAM sensing based implementation, compared to the 90 snapshots required for sensing procedure in hiePM to ensure zero RMSE (i.e., no misalignment) for the beam alignment problem.

2) RMSE as a function of SNR, α unknown scenario: In Fig. 3 (b), we plot the RMSE (over $Q = 100$ realizations) in u-space as a function of SNR in dB. Both α and u are unknown unless otherwise specified. The proposed (adaptive) SVAM-based sensing and estimation recovers u on grid. The proposed (adaptive) SVAM-based sensing and detection strategy decides between two partitions ($P = 2$). The 2 partitions are steered together to identify partitions with the largest power difference. The hiePM curves are based on the work in [4], [17]. The blue dashed curve for hierarchical posterior matching assumes a fixed prior of $\mathcal{CN}(\alpha, 1)$ i.e., it assumes the mean is set to correct α. As expected, when the SNR is low, the prior is more important and further helps to improve the estimation performance. At high SNR, the prior is less effective. As observed, simply replacing the sensing in hiePM with SVAM improves the performance (red curve) indicating the effectiveness of proposed sensing. With α-unknown, the proposed sensing improves over the hiePM with fixed prior curve. Also, as observed, the detection strategy replaces the estimation strategy at low SNR. At high SNR, or after reliable detection, an estimation strategy may be used over the detection algorithm.

V. Conclusion

A novel sensing approach named as Synthesis of Virtual Array Manifold (SVAM) is proposed for mmWave single RF chain systems and the ensuing benefits are discussed. SVAM offers a flexible framework for sensing and allows for inference using *digital* filtering on the synthesized virtual array. Several algorithms for initial alignment are discussed, including a modified hierarchical posterior matching-based algorithm. The significance of the SVAM sensing for initial alignment is empirically studied. SVAM sensing enables highly informative measurements and can be easily integrated into existing algorithms for initial alignment.

References

[1] A. Ghosh, A. Maeder, M. Baker, and D. Chandramouli, "5G evolution: A view on 5G cellular technology beyond 3GPP Release 15," *IEEE Access*, vol. 7, pp. 127639–127651, 2019.

[2] C.H. Doan, S. Emami, D.A. Sobel, A.M. Niknejad, and R.W. Brodersen, "Design considerations for 60 GHz CMOS radios," *IEEE Communications Magazine*, vol. 42, no. 12, pp. 132–140, 2004.

[3] F. Liu, Y. Cui, C. Masouros, J. Xu, T. X. Han, Y. C. Eldar, and S. Buzzi, "Integrated sensing and communications: Toward dual-functional wireless networks for 6G and beyond," *IEEE Journal on Selected Areas in Communications*, vol. 40, no. 6, pp. 1728–1767, 2022.

[4] S. Chiu, N. Ronquillo, and T. Javidi, "Active learning and CSI acquisition for mmwave initial alignment," *IEEE Journal on Selected Areas in Communications*, vol. 37, no. 11, pp. 2474–2489, 2019.

[5] H. L. V. Trees, "Optimum array processing: Part IV of Detection, Estimation, and Modulation Theory," *John Wiley & Sons, Ltd*, 2002.

[6] C. Waldschmidt, J. Hasch, and W. Menzel, "Automotive radar-from first efforts to future systems," *IEEE Journal of Microwaves*, vol. 1, 2021.

[7] R. R. Pote and B. D. Rao, "Reduced dimension beamspace design incorporating nested array for mmwave channel estimation," in *53rd Asilomar Conference on Signals, Systems, and Computers*, 2019.

[8] A. Alkhateeb, O. El Ayach, G. Leus, and R. W. Heath, "Channel estimation and hybrid precoding for millimeter wave cellular systems," *IEEE Journal of Selected Topics in Signal Proc.*, vol. 8, no. 5, Oct 2014.

[9] A. V. Oppenheim and R. W. Schafer, *Discrete-Time Signal Processing*, Prentice Hall Press, USA, 3rd edition, 2009.

[10] R. Schmidt, "Multiple emitter location and signal parameter estimation," *IEEE Transactions on Antennas and Propagation*, vol. 34, no. 3, 1986.

[11] R. Roy and T. Kailath, "ESPRIT-estimation of signal parameters via rotational invariance techniques," *IEEE Transactions on Acoustics, Speech, and Signal Processing*, vol. 37, no. 7, pp. 984–995, 1989.

[12] R. R. Pote and B. D. Rao, "Maximum likelihood-based gridless DoA estimation using structured covariance matrix recovery and sbl with grid refinement," *IEEE Trans. on Signal Proc.*, vol. 71, pp. 802–815, 2023.

[13] A. Moffet, "Minimum-redundancy linear arrays," *IEEE Transactions on Antennas and Propagation*, vol. 16, no. 2, pp. 172–175, 1968.

[14] P. Pal and P. P. Vaidyanathan, "Nested arrays: A novel approach to array processing with enhanced degrees of freedom," *IEEE Transactions on Signal Processing*, vol. 58, no. 8, pp. 4167–4181, 2010.

[15] X. Zhang, A.F. Molisch, and S. Y. Kung, "Variable-phase-shift-based RF-baseband codesign for mimo antenna selection," *IEEE Transactions on Signal Processing*, vol. 53, no. 11, pp. 4091–4103, 2005.

[16] R. R. Pote, "Efficient techniques for millimeter wave sensing and beam alignment, sparse recovery, and DoA estimation," in *Ph.D. dissertation, University of California, San Diego*, 2023.

[17] N. Ronquillo, S. Chiu, and T. Javidi, "Sequential learning of CSI for mmwave initial alignment," in *2019 53rd Asilomar Conference on Signals, Systems, and Computers*, 2019, pp. 1278–1283.